Validating FOXO4 as a therapeutic target for protecting against ischemia-reperfusion-caused neuronal injury

Yasin Asadi, Frahad Gorjipour, Anand Chakroborty, Rozenn K. Moundounga, Abena Dwamena, Erin Gilstrap, and Hongmin Wang*

Department of Pharmacology and Neuroscience, Garrison Institute on Aging, and Center of Excellence for Translational Neuroscience and Therapeutics, Texas Tech University Health Sciences Center (TTUHSC), School of Medicine, Lubbock, Texas 79430-6592, USA.

***Corresponding author:**

Hongmin Wang, Ph.D., Professor, Department of Pharmacology and Neuroscience, Texas Tech University Health Sciences Center (TTUHSC), School of Medicine, Lubbock, Texas 79430-6592, USA. Tel: +18067437089, Email: Hongmin.Wang@ttuhsc.edu

Abstract:

Background: Previous data suggest that in the conditions of I/R in mice and the oxygen-glucose deprivation (OGD) in cell cultures, FOXO4 facilitates inflammation and oxidative stress in *non-brain tissues*, indicating that downregulation of FOXO4 may be neuroprotective in I/R-induced injury in the brain. However, this possibility has not been tested in the cerebral I/R condition.

Method: FOXO4 knockout (KO) and wild-type (WT) primary neuronal cultures were treated with an oxidative stress inducer, menadione (MD), or OGD, and then cell viability was assessed via ATP and MTT assays. The KO and WT mice at 2-3 months were subjected to one-hour (h) transient middle cerebral artery occlusion (tMCAO). Mice were sacrificed after 24 h for TTC staining or after 48 h for immunohistochemical staining. Alternatively, animals were allowed to survive 1-10 days after tMCAO to test their functional recovery. Furthermore, using a structure-based approach combined with cell-based assays, we screened FOXO4 inhibitors and identified actinomycin D (ActD) as a potent FOXO4 inhibitor. We also tested the therapeutic role of ActD in both *in vitro* and *in vivo* models of ischemic stroke.

Result: KO of FOXO4 reduced the infarct volume, improved animal survival, decreased neurological deficits, and enhanced functional recovery compared to WT mice. Immunohistochemical staining of astrocytes and microglia revealed that KO brains showed a reduced number of astrocytes and microglia in the peri-infarcted area two days after I/R. Western blot analysis of proinflammatory cytokines, IL-1β, IL-6, and TNF-α, indicated decreased levels of proinflammatory cytokines two days following I/R. The identified FOXO4 inhibitor, ActD, attenuated oxidative stress- and OGD-induced neuronal death. ActD also reduced neuronal injury of the brain and enhanced functional recovery in WT mice following tMCAO.

Conclusion: We conclude that disrupting FOXO4 is neuroprotective and the identified inhibitor, ActD, may be a therapeutic agent for treating ischemic stroke-induced brain injury.

Keywords: FOXO4; stroke; neuroinflammation; ischemia; reperfusion; transient middle cerebral artery occlusion; inhibitor; therapy; functional recovery

Introduction

Stroke is a major health problem: it is the fifth leading cause of death and the leading cause of disability in the United States. Ischemic stroke is the most frequent type of stroke, affecting millions of people across the globe.[1] Despite intensive research, there is still no effective treatment for this condition, and tissue plasminogen activator remains the only Food and Drug Administration-approved medication for treating ischemic stroke.[2] While it is necessary to restore cerebral blood flow, reperfusion itself induces the production of large amounts of reactive oxygen species that further damage proteins and other intracellular macromolecules to exacerbate brain injury.[3] Moreover, ischemia/reperfusion (I/R) also disrupts the blood-brain barrier, resulting in infiltration of leukocytes and inflammatory responses to aggravate brain injury.[4] To develop effective therapeutics, it is necessary to identify and validate additional therapeutic targets.

Transcriptional gene regulation, governed primarily by numerous transcriptional factors, is one of the upstream parts potentially modulating I/R-induced brain injury. The Forkhead Box Proteins O (FOXOs), consisting of four structurally and functionally related proteins, FOXO1 (also referred to as FKHR), FOXO3 (also known as FOXO3a), FOXO4 (also known as AFX1), and FOXO6, are one family of transcription factors, representing mammalian homologs of daf-16 in *C. elegans* and playing a crucial role in cell survival, cell proliferation, metabolism, response to oxidative stress, apoptosis, and aging.[5] Under oxidative stress or the absence of the cellular survival drive of growth factors, FOXOs translocate to the nucleus and upregulate a series of target genes, thereby promoting cell growth arrest and apoptosis.[6,7]

Despite the highly structural and functional similarities of FOXOs, previous data have suggested that the physiological roles of FOXOs are functionally diverse in mammals.[8,9] For instance, FOXO1 deficiency is embryonically lethal and FOXO3 deficiency exhibits age-dependent infertility in females in mice; however, the loss of FOXO4 does not cause any notable changes in the mouse, suggesting that FOXO4 may play a different role from other FOXO members.[8,10] FOXO4 was found to promote cell death in the heart and the liver following I/R, while downregulation of FOXO4 confers protection against I/R-induced tissue injuries in these organs.[11,12] Moreover, following cardiac ischemia, FOXO4 enhances the interaction of leukocytes with the endothelial cells of blood vessels to promote early tissue inflammation.[13] In contrast, downregulation of FOXO4 suppresses oxidative stress-induced cell death in proangiogenic cells and promotes neovascularization in ischemic limbs.[14] Functionally, FOXO activity is negatively regulated by phosphorylation via the phosphoinositide 3-kinase-Akt pathway, a well-known cell survival pathway.[6,7] Ischemic pre-conditioning upregulates Akt activity, leading to FOXO inhibition and promotion of neuronal survival against a subsequent severe ischemic insult.[15] These prior studies suggest that FOXO4 may be a therapeutic target for ischemic stroke, yet this has not been tested. In this study, we examined the role of FOXO4 in neuronal injury *in vitro* and *in vivo* following oxidative stress, oxygen-glucose deprivation (OGD), and I/R, using the primary neuronal cultures and FOXO4 knockout (KO) mice combined with different approaches.

Materials and Methods

Mice

All animal-related experiments and procedures were approved by the Institutional Animal Care and Use Committee of the Texas Tech University Health Science Center and were in compliance

with the National Institute of Health Guide for the Care and Use of Laboratory Animals. Animals were maintained on a 14-/10-hour light/dark cycle with a maximum of four mice per cage able to access water and food ad libitum. FOXO4 global knockout (KO) mice in the background of FVB have been described before[13] and were used for ischemic stroke-induced brain infarct studies, while the same strain of wild-type (WT) mice was used as the control. For animal behavioral studies, the KO and WT male mice with a hybrid background (F1 generation) produced from the heterozygous KO FVB females crossed with the WT C57BL/6 males were used, because of the retina degeneration problem in the FVB mice. As FOXO4 is an X chromosome-linked gene, in this breeding strategy, 50% of males would be FOXO4 KO males and 50% would be WT males that were used as controls for behavioral studies following ischemic stroke. More than one litter of animals was used in each experiment. The male animals between 8–12 weeks of age with a body weight of 25-30 g were used in the study. Sample size calculations and power analysis were performed according to our previously described methods[16] using the statistical software Stata (StataCorp LP, College Station, TX, USA).

Primary neural cell culture

Primary cortical neuronal cultures were prepared from wild-type and FOXO4 KO mice at postnatal day 0 according to our previously described methods.[17] Briefly, the cerebral cortex was isolated and digested with 5 ml of 0.25% trypsin/EDTA supplemented with 75 µl 0.1% DNase (2000 UI/mg). After 15-20 minutes of digestion at 37°C, the digested tissues were centrifuged at 1000 × g for 3 minutes at room temperature. The supernatant was discarded, and the resulting tissue pellets were resuspended with fetal bovine serum (FBS) to stop the digestion. After centrifugation, the tissues were resuspended with primary neuronal culture medium (Neurobasal medium supplemented with 2% B27, 2 mM L-glutamine, and penicillin/streptomycin) and then pipetted up and down several times using serological pipets to disrupt tissues. After filtering through a 70 µm nylon cell strainer, the cell suspension was adjusted and plated in poly-DL-lysine-coated 12-well plates. After 7 days of incubation at 37°C in a 5% CO2 incubator, the cells were treated with 20 µM menadione (MD) for 24 h or oxygen-glucose deprivation (OGD) for 3 h and then in normal culture condition for 21 h in the absence or presence of an identified FOXO4 inhibitor, actinomycin D (ActD, 0.1 µM).

Oxygen-glucose deprivation (OGD)

WT and FOXO4 KO primary neuronal cultures were subjected to OGD at 7-10 *in vitro* days according to previous methods.[17] Briefly, the neuronal culture medium was replaced with a glucose-free Hank's Balance Salt Solution (HBSS) and then the culture plates were placed into a hypoxic chamber where the air was replaced with a 5% N_2 and 95% CO_2. After 3 h of OGD condition, the neuronal cultures were returned to the normal culture condition, and after 21 h cell viability was measured via ATP and MTT assays.

ATP assay

We used an ATP detection kit (Cayman Chemical, Ann Arbor, Michigan, USA) to measure ATP levels in cultured neurons according to the manufacturer's instructions.

MTT assay

Cell viability in cell cultures was assessed using an MTT assay kit (R&D Systems, Minneapolis, MN, USA) based on the company's guide.

Transient middle cerebral artery occlusion (tMCAO)

The tMCAO procedure was performed according to previously described methods.[18,19] Briefly, anesthesia of mice was induced with 5% isoflurane and then maintained with 2% isoflurane. The left hemisphere was subjected to tMCAO using a silicon-coated monofilament (RWD, Sugar Land, TX, USA) and after 1 hour, the monofilament was removed. A Laser Speckle Imaging System (RWD, Sugar Land, TX, USA) was used to monitor cerebral blood flow through MCA. Only the mice with successful occlusion of MCA were included in the studies, as reflected by reduced blood flow by over 80% and reperfusion with more than 75% recovery of blood flow in the MCA.

Drug treatment of mice

For drug treatment studies, WT males were randomly separated into the vehicle group and drug treatment group using an online tool (http://www.graphpad.com/quickcalcs/). Either 0.25 or 0.5 mg/kg of actinomycin D or vehicle was intraperitoneally injected into WT 1 h before tMCAO. After 24 h, mice were euthanized to collect the brains for TTC staining. Alternatively, the mice were allowed to survive for 1-10 days to assess functional recovery.

TTC staining and measurement of infarct volumes

Mice were euthanized 24 h after I/R to isolate the brains. After being sectioned into 2 mm slices, the brain sections were incubated with 2% of 3,5-triphenyl tetrazolium chloride (TTC, Sigma, Saint Louis, MO, USA) at 37°C for 20 minutes. Subsequently, the sections were fixed in 4% paraformaldehyde and then imaged. The infarcted volume was measured using Image J software and calculated as previously described.[20]

Assessment of modified neurological deficits

At 1, 3, 5, and 7 days following I/R, a modified neurological severity score (mNSS) system was applied to assess the motor and sensory functions in mice.[21] Based on this system, a scale of 0 to 14 was given to an animal, with 0 for normal neurological behavior and 14 for the maximal neurological deficit.[22]

Novel object recognition (NOR) test

A box (50 × 50 × 30 cm) containing two objects was used for the NOR test at 7 days following I/R. On the first day of the test, mice were placed in the box and allowed to move freely for 10 minutes. On the second day, one of the objects was replaced with a new one (novel object), and the other remained as a familiar object. Then, mice were placed into the box to move and explore the objects. By using a camera, the total time spent exploring each object was recorded, and the ratio of the new object exploration was calculated as the discrimination index (DI = (Tnovel - Tfamiliar)/(Tnovel + Tfamilar).[19]

Y-maze test

In the training session, each mouse was placed in an arm of the Y maze (start arm) with one of the arms blocked with an opaque door (novel arm) and allowed to explore the start arm and remaining arm (other arm) for 5 minutes. The mouse was then removed and returned to its home cage, and the novel arm was unblocked. After one hour, in the test trial, the mouse was replaced on the start arm and allowed to explore all three arms freely for 2 minutes. The number of arm entries was recorded by the experimenter blind to the genotype of the mice.

Immunofluorescent staining

Brains were coronally cut into 3 parts and the frontal and occipital parts were used for TTC staining to define the penumbral area. The middle part was washed and fixed in 4% paraformaldehyde. Then, the 16 μm thickness sections were prepared on a Cryostat (Leica, Buffalo Grove, IL, USA), and the brain sections were processed based on the prior method.[23] The primary antibodies used were anti-GFAP (1:50, EMD Millipore, #MAB360), anti-Iba1 antibody (1:50, Cell Signaling Technology, #31659), anti-CD45 (Invitrogen #MA180090), anti-Ly6G (Cell Signaling #87048), and anti-CD11 (Developmental Studies Hybridoma # M1/70.15.11.5.2). The secondary antibodies were Texas red-conjugated anti-rabbit and FITC-conjugated anti-mouse antibodies. DAPI (IHC-tek#IW-1404) was used to stain the nuclei.

The images were captured with a fluorescence microscope (Echo Revolve, San Diego, USA) and quantified with Image J software.[24] The ratio of the red- or green-positively stained cells in each field was calculated by the total red or green cells divided by the total number of cells (DAPI positively stained cells).[25,26]

Western blot

The cortex of the left (i.e. the I/R side) hemisphere of each mouse brain was collected for lysate preparation in the RIPA buffer supplemented with a protease cocktail. The brain tissues were sonicated in the lysate buffer and the lysates were centrifuged at 12,000 x g for 4 min at 4°C. The supernatant was collected and then the total protein concentration was measured before being subjected to the SDS-PAGE and transferred to the nitrocellulose membrane according to previous methods.[17] The antibodies used were anti-IL-1β (1:1000, Cell Signaling, #63124), anti-IL-6 (1:1000, Cell Signaling, #12912), anti-TNFα (1:1000, Cell Signaling, #11948), and anti-β-actin (1:1000, Santa Cruz Biotechnology, #sc-1616). The secondary antibodies used were anti-rabbit IgG, HRP-conjugated antibody (Cell Signaling, #7074), and anti-mouse IgG, HRP-conjugated antibody (Cell Signaling, #7076). The western blot results were documented using an imaging system (C400 Azure Biosystem), and protein band intensities were measured using the NIH Image J software.

Structure-based drug screening

We utilized the Autodock Vina in the PyRx 0.9.8 software (https://pyrx.sourceforge.io/) to perform the docking-based virtual screening of several small compound libraries against FOXO4

DNA-binding domain (DBD, Protein Data Bank, https://www.rcsb.org/; PDB: 3L2C), with a grid box of 20 x 20 x 20 Å positioned within the box center coordinates -1.0, 13.0 and -15.0 focusing on the DBD of FOXO4. The FOXO4 DBD was modified by removing the DNA chains during computational analyses. We screened 7,742 compounds from four different chemical libraries, including the NIH Clinical Collections https://pubchem.ncbi.nlm.nih.gov/source/NIH%20Clinical%20Collection), the FDA-approved and clinical drugs (https://www.targetmol.com/library-collection-2/sorted-by-clinical-phase and https://www.apexbt.com/ discoveryprobetm-clinical-fda-approved-drug-library.html), and a natural product library (https://www.apexbt. com/discoveryprobetm-natural-product-library-plus-1.html). The lead compounds were then docked onto FOXO1 DBD (PDB: 3COA) and FOXO3 DBD (PDB: 2UZK) and any candidates that also showed a high affinity to FOXO1 or FOXO3 were eliminated from the list.

Cell-based reporter assay

HEK293 cells expressing a human FOXO4 plasmid (Addgene #17549)[27] and a luciferase reporter plasmid (Addgene, # 34571) driven by a FOXO4 target gene Arginase-1 promoter[13,28], were treated with triplates with 100 nM of identified compounds or vehicle (DMSO) for 8 h and the treated cells were then subjected to a luciferase-based reporter assay using a luciferase reporter substrate kit (Abcam, Waltham, MA, USA). Moreover, to eliminate the compounds that also showed inhibitory effect on FOXO1 and FOXO3, we performed additional reporter assays with HEK293 cells co-transfected with the 3XIRS luciferase (Luc) reporter that contains 3 copies of the insulin-responsive sequence[29] or FHRE-Luc[30] together with FOXO3 plasmid (Addgene #8360)[30].

Molecular docking

We used SMILES[31] notation for ActD (CHEMBI: 27666) ligand against the FOXO4 (PDB: 3L2C) to predict the protein-ligand binding sites in SwissDock 2024[32] and Protenix (https://protenix-server.com/add-prediction), keeping multiple sequence alignment and seed 95326 as a parameter. AutoDock Vina has applied a method for SwissDock, a grid box of 20 x 20 x 20 Å positioned within box center coordinates -1.0, 13.0, and -15.0 focusing on the DNA-binding domain of FOXO4 for accurate docking predictions of actinomycin D. The PDB model

(3L2C) was modified by removing the DNA chains during compuational analyses. A separate analysis was executed with the matching coordinates keeping Attracting Cavities for higher confidence predictions in SwissDock. The results were visualized using UCSF ChimeraX[33] on Macintosh System.

Statistical analysis

Statistical analyses were conducted using GraphPad Prism version 9.0 statistical software. Differences between the two groups were assessed using an unpaired t-test. For comparisons between different groups of animals in the RAWM, repeated measures, and two-way ANOVA with Tukey's post hoc test were utilized. All numerical data were presented as mean ± SD or SEM. $P < 0.05$ was regarded as statistically significant.

Results

KO of FOXO4 reduces neuronal death caused by oxidative stress and OGD in primary cortical neuronal cultures

To assess the effect of KO of FOXO4 on oxidative stress-induced cell death, we treated the primary cortical neuronal cultures with an oxidative stress inducer, menadione (MD)[18], and then measured the viability of the cells via ATP and MTT assays. Our results indicated that the KO neurons showed increased cell survival as reflected by higher ATP levels in KO cells compared to WT cells (**Fig. 1a**). Increased viability in the KO cells was also supported by the MTT assay (**Fig. 1b**). However, in those neuronal cultures without MD treatment, the cellular viability did not differ between WT and KO neurons (**Fig.1a, 1b**). To validate these results, we further treated the two types of cultured neurons with an *in vitro* model of ischemic stroke, OGD, and then examined cell viability. In both the ATP assay (**Fig. 1c**) and MTT assay (**Fig. 1d**), KO neurons showed reduced cell death compared to WT neurons. These results indicate that KO of FOXO4 is neuroprotective against oxidative stress- and OGD-induced neuronal death.

KO of FOXO4 reduces the infarct volume and enhances functional recovery after tMCAO

To determine whether FOXO4 influences the outcome of I/R-induced brain injury *in vivo*, we performed tMCAO to FOXO4 KO and WT mice and after 24 h following the reperfusion, mice

were euthanized to assess brain injury by the TTC staining (**Fig. 2a**). Our results showed a significant decrease in infarct volume in the KO group compared to the WT group (**Fig. 2b, 2c**), suggesting that disrupting the FOXO4 gene is neuroprotective against I/R-induced neuronal injury.

To determine whether KO of the FOXO4 influences animal survival following I/R, animal death, and survival were recorded on days 1, 2, 3, 4, 5, and 7 after tMCAO. As shown in **Fig. 2d,** KO of FOXO4 increases animal survival rate. Moreover, we also assessed the neurological deficits and found that KO of FOXO4 facilitated animal functional recovery, as reflected by the reduced mNSSs compared to the WT mice following the tMCAO procedure on days 1, 3,5, and 7 (**Fig. 2e**). Improved functional recovery in the KO mice was also supported by the cognitive function test, including the memory capabilities that were evaluated 10 days after MCAO. We observed better learning and memory in the KO mice compared to WT mice in the NOR test (**Fig. 2f**). Therefore, KO of FOXO4 reduces neuronal death, improves animal survival, and enhances functional recovery following I/R.

KO of FOXO4 attenuates neuroinflammation in the brain following I/R

Neuroinflammation is a hallmark following I/R in the brain. To assess whether KO of FOXO4 alters the inflammatory responses, brain tissues on the ipsilateral side were isolated from KO and WT mice 48 h after I/R. Western blot analysis of the pro-inflammatory cytokines, including TNF-α, IL-1β, and IL-6, revealed a significant reduction in the KO brains compared to WT brains (**Fig. 3a-3d**). These data indicate that KO of FOXO4 attenuates I/R-induced neuroinflammation.

KO of FOXO4 suppresses activation of astrocytes and microglia in the brain following I/R

To assess the reactive astrocytes and microglia, we performed immunostaining of the astrocyte marker, GFAP (glial fibrillary acidic protein), and microglia marker, Iba1 (ionized calcium-binding adaptor molecule 1) to the mouse brain 48 h following I/R. As shown in **Fig. 4**, the numbers of GFAP and Iba1 positively stained cells were significantly reduced in the KO brain compared to the WT brain, suggesting that the KO of FOXO4 suppresses the activation of astrocytes and microglia.

KO of FOXO4 reduces leukocyte infiltration in the brain following I/R

Another pathological feature following I/R is the infiltration of leukocytes in the brain. To determine the leukocyte infiltration, the brain sections were immunohistochemically stained either with the CD45 (a marker for the total hematopoietic cells), CD11b (a marker for macrophages, granulocytes, and NK cells), or Ly6G *(*a marker for monocytes, granulocytes, and neutrophils). As shown in **Fig. 5a** and **5b**, the number of the CD45 positively stained cells in the KO brain showed a reduction trend compared to the WT brain, despite the lack of statistical difference between the two groups. In contrast, the number of positively stained CD11b was significantly decreased (**Fig. 5c** and **5d**) in the KO brain compared to the WT brain. Similarly, the number of positively stained Ly6G (leukocytes) was also significantly decreased (**Fig. 5e** and **5f**) in the KO brain compared to the WT brain. These data indicate that KO of FOXO4 attenuates leukocyte infiltration.

Identification of Actinomycin D as a FOXO4 inhibitor

The results demonstrated above strongly suggest that disrupting FOXO4 function is beneficial for neuronal survival following oxidative stress or I/R. To translate the results into potentially clinical treatments, we identified compounds that could directly inhibit the interaction between FOXO4 and its DNA substrate. The crystal structure of the FOXO4 protein is unavailable; however, the 1.9 Å resolution 3D crystal structure of the DNA-binding domain (DBD, amino acid sequence 93-196) of human FOXO4 bound to a 103 bp DNA duplex has been reported (**Fig. 6a**).[34] Additionally, human FOXO4 DBD is identical to mouse FOXO4. We utilized this FOXO4 DBD and performed virtual docking of several small molecular libraries against FOXO4 DBD (Protein Data Bank, PDB: 3L2C). The top-scoring compounds were then docked onto FOXO1 DBD (PDB: 3COA) and FOXO3 DBD (PDB: 2UZK) and any candidates that also showed a high affinity to FOXO1 or FOXO3 were eliminated from the list. This led to Actinomycin D (ActD), an FDA-approved antibiotic, as one of the top candidates (**Fig. 6b**). ActD is used for chemotherapy to treat many different types of cancer[35] and was the first natural antibiotic found to have anti-cancer activity[36].

In a cell-based reporter assay, ActD showed significant inhibitor activity against FOXO4 (**Fig. 6c**). Structurally, FOXO4 DBD is more similar to FOXO3 DBD than to FOXO1 DBD[37]. However, our reporter assay revealed that ActD did not inhibit FOXO3 activity at the same concentration (0.1 μM) (**Fig. 6d**).

The results of computational protein-ligand docking advocated helix H3 as the major site of inhibition (**Fig. 6e, 6f**). SwissDock-based AutoDock Vina execution exhibited active residues Arg78, His79 and Ser82 interacting with ActD (**Fig. 6g**). AlphaFold3-based Protenix[38] predicted similar heavy atom contacts with ligand to H2 (Leu47), H3 (Asn75, Arg78, His79, Ser82 and Leu83) and S3 (Lys89) domains of FOXO4 (**Fig. 6h**). It is important to note that the sequential numbering of these receptor residues is based on the active DBD of FOXO4 and does not correspond to the entire protein from the N to C terminal. Interaction of ActD with Arg78 is crucial as two hydrogen bonds are indicated (**Fig. 6g**) with donor-acceptor distances of 3.480 Å (NH_2) and 3.451 Å (NE), whereas the distance between ActD to Ser82 and Lys89 is 2.735 Å and 3.334 Å (**Fig. 6g, 6h**), respectively. The corresponding seven fundamental amino acid residues bound to the ligand are L124, N152, R155, H156, S159, L160, and K166 for FOXO4.

Pharmacological blockage of FOXO4 attenuates oxidative stress- and OGD-induced neuronal death *in vitro*

To determine the effect of ActD on primary neuronal cultures in response to oxidative stress, we treated cultured neurons with MD in the presence of 0.1 μM ActD. Both ATP assay (**Fig. 7a**) and MTT assay results (**Fig. 7b**) indicated a protective effect of ActD on MD-induced cell death. Likewise, ActD also protected neurons from OGD-caused neuronal death, as shown by increased ATP level (**Fig. 7c**) and neuronal survival rate (**Fig. 7d**), suggesting that ActD attenuates oxidative stress- and OGD-induced neuronal death *in vitro*.

Treating WT mice with ActD reduces tMCAO-induced brain injury and promotes functional recovery

To further assess the therapeutic effect of ActD on I/R-induced brain injury in mice following tMCAO, we treated WT mice with ActD (0.25 or 0.5 mg/kg, i.p.) or vehicle 1 h before tMCAO (**Fig. 8a**). Following 1 h of ischemia and 24 h reperfusion, mice were sacrificed for TTC staining (**Fig. 8b**). Our data showed that ActD treatment significantly reduced I/R-induced brain injury at 0.5 mg/kg (**Fig. 8b, 8c**). Moreover, ActD treatment also enhanced the animal function recovery, as shown by reduced mNSS scores (**Fig. 8d**) and increased cognitive function reflected by the Y-maze test compared to the vehicle treatment. These data indicate that ActD is neuroprotective against I/R-induced brain injury.

Discussion

In this study, we investigated the role of FOXO4 in oxidative stress-, OGD-, and cerebral I/R-induced neuronal injury and validated that FOXO4 is a therapeutic target. Moreover, we identified ActD as a FOXO4 inhibitor that showed a therapeutic effect on neurons following oxidative stress, OGD, or I/R insults. While the protective role of FOXO4 in non-neuronal cells/tissues was previously reported *in vitro* and *in vivo*[39-41], to our knowledge, this is the first study of FOXO4 in I/R-induced neuronal injury in neurons and animal brains.

Unlike FOXO1 KO mice, which are embryonic lethal[42], FOXO4 KO mice do not differ from their WT littermates. Our findings revealed that KO of FOXO4 yielded a better outcome after cerebral I/R, significantly reducing the infarct volume 24 h after I/R, and improving functional recovery after that. KO of FOXO4 also enhanced learning and memory capability in mice after one week following the I/R. To understand possible mechanisms, we found that the FOXO4 KO mice showed a significant decrease in inflammatory cytokines in the brain cortex 48 h after I/R. The inflammatory cytokines come from two sources, immune cells attracted from systemic circulation, and locally activated glial cells.[43] Since we observed a significant decrease in CD11- and Ly6G-positive cells in the KO brain following I/R, leukocyte infiltration in the FOXO4 KO brain was reduced. Since CD11b is highly expressed by myeloid cells, the first line in the immune response[44], the significant decrease in CD11b in the FOXO4 KO brain should reflect reduced leukocyte infiltration through the microvessels.

Additionally, our results also support reduced activation of local microglia and astrocytes in the KO compared to the WT mouse brain. These findings are in good accordance with previous data showing the anti-inflammatory effect of deleting FOXO4 in an ischemic condition in another organ *in vivo*[45], and in cerebral endothelial cells in an *in vitro* model of I/R.[39] After I/R, ROS, cell debris, mitochondrial dysfunction, excitotoxicity, and disrupted blood-brain barrier (BBB) work together to trigger inflammatory responses, involving both local and systemic immune factors. As a transcription factor, FOXO4 regulates many pathological processes, such as apoptosis, endothelial function, ROS production, and BBB integrity to facilitate cell death, whereas KO of FOXO4 leads to neuroprotective effects and impeding the

progression of neuronal death and infarction, ultimately preserving functional performance, as supported by our findings.

Although DBDs of transcription factors were generally considered "undruggable" due to their relatively flat and similar surface areas.[46] However, recent studies have challenged this interdiction by developing an improved *in-silico* screening approach to eliminate potential non-selective inhibitors.[47] For instance, the identified top-scoring compounds targeting the STAT3 DBD from an in-silico screening of a chemical library were docked onto the STAT1 DBD[48,49]. Any compounds predicted to also bind to the STAT1 DBD were eliminated due to potential lack of selectivity and this improved approach helped the authors identify a STAT3-selective hit molecule.[49] Using a similar strategy, we identified a FOXO4 inhibitor, ActD, which could be potentially specific for FOXO4, because our results suggest that it did not suppress FOXO3 activity at the same concentration *in vitro*. Importantly, ActD confers neuroprotection against oxidative stress- and OGD-induced neuronal death in the primary neuronal cultures reduces infarct volume, and enhances functional recovery following I/R in the brain of mice. These data suggest that ActD may be used as a therapeutic to treat the disease.

In conclusion, using a genetically modified mouse combined with primary neuronal cultures and other approaches, we validated FOXO4 as a therapeutic target for I/R-induced brain injury. Our data suggest that KO of FOXO4 reduces neuronal injury, promotes functional recovery, suppresses leukocyte infiltration, and attenuates neuroinflammation. Moreover, we also identified ActD as a therapeutic for I/R-induced neuronal death, which has the potential to be used in the clinic to treat acute ischemic stroke or other neurological disorders.

Acknowledgments: This work was supported by NIH/NINDS NS124846. Any opinions, findings, conclusions, or recommendations expressed in this material are those of the authors and do not necessarily reflect the views of the NIH.

Conflicts of Interest: The authors declare no conflicts of interest.

References

1. Ananth CV, Brandt JS, Keyes KM, Graham HL, Kostis JB, Kostis WJ. Epidemiology and trends in stroke mortality in the USA, 1975–2019. *International journal of epidemiology*. 2023;52:858-866.
2. Baird AE, Jackson R, Jin W. Tenecteplase for acute ischemic stroke treatment. Paper/Poster presented at: Seminars in Neurology; 2021;
3. Sun MS, Jin H, Sun X, Huang S, Zhang FL, Guo ZN, Yang Y. Free Radical Damage in Ischemia-Reperfusion Injury: An Obstacle in Acute Ischemic Stroke after Revascularization Therapy. *Oxid Med Cell Longev*. 2018;2018:3804979. doi: 10.1155/2018/3804979
4. Jiang X, Andjelkovic AV, Zhu L, Yang T, Bennett MVL, Chen J, Keep RF, Shi Y. Blood-brain barrier dysfunction and recovery after ischemic stroke. *Prog Neurobiol*. 2018;163-164:144-171. doi: 10.1016/j.pneurobio.2017.10.001
5. Maiese K. Forkhead Transcription Factors: Formulating a FOXO Target for Cognitive Loss. *Curr Neurovasc Res*. 2017;14:415-420. doi: 10.2174/1567202614666171116102911
6. Storz P. Forkhead homeobox type O transcription factors in the responses to oxidative stress. *Antioxid Redox Signal*. 2011;14:593-605. doi: 10.1089/ars.2010.3405
7. Farhan M, Wang H, Gaur U, Little PJ, Xu J, Zheng W. FOXO Signaling Pathways as Therapeutic Targets in Cancer. *Int J Biol Sci*. 2017;13:815-827. doi: 10.7150/ijbs.20052
8. Hosaka T, Biggs WH, 3rd, Tieu D, Boyer AD, Varki NM, Cavenee WK, Arden KC. Disruption of forkhead transcription factor (FOXO) family members in mice reveals their functional diversification. *Proc Natl Acad Sci U S A*. 2004;101:2975-2980. doi: 10.1073/pnas.0400093101
9. Wang M, Zhang X, Zhao H, Wang Q, Pan Y. FoxO gene family evolution in vertebrates. *BMC Evol Biol*. 2009;9:222. doi: 10.1186/1471-2148-9-222
10. Castrillon DH, Miao L, Kollipara R, Horner JW, DePinho RA. Suppression of ovarian follicle activation in mice by the transcription factor Foxo3a. *Science*. 2003;301:215-218. doi: 10.1126/science.1086336
11. Yu L, Zhang W, Huang C, Liang Q, Bao H, Gong Z, Xu M, Wang Z, Wen M, Cheng X. FoxO4 promotes myocardial ischemia-reperfusion injury: the role of oxidative stress-induced apoptosis. *Am J Transl Res*. 2018;10:2890-2900.
12. He B, Yang F, Ning Y, Li Y. Sevoflurane alleviates hepatic ischaemia/reperfusion injury by up-regulating miR-96 and down-regulating FOXO4. *J Cell Mol Med*. 2021;25:5899-5911. doi: 10.1111/jcmm.16063
13. Zhu M, Goetsch SC, Wang Z, Luo R, Hill JA, Schneider J, Morris SM, Jr., Liu ZP. FoxO4 promotes early inflammatory response upon myocardial infarction via endothelial Arg1. *Circ Res*. 2015;117:967-977. doi: 10.1161/CIRCRESAHA.115.306919
14. Nakayoshi T, Sasaki K, Kajimoto H, Koiwaya H, Ohtsuka M, Ueno T, Chibana H, Itaya N, Sasaki M, Yokoyama S, et al. FOXO4-knockdown suppresses oxidative stress-induced apoptosis of early pro-angiogenic cells and augments their neovascularization capacities in ischemic limbs. *PLoS One*. 2014;9:e92626. doi: 10.1371/journal.pone.0092626
15. Zhan L, Wang T, Li W, Xu ZC, Sun W, Xu E. Activation of Akt/FoxO signaling pathway contributes to induction of neuroprotection against transient global cerebral ischemia by hypoxic pre-conditioning in adult rats. *J Neurochem*. 2010;114:897-908. doi: 10.1111/j.1471-4159.2010.06816.x
16. Liu Y, Min JW, Feng S, Subedi K, Qiao F, Mammenga E, Callegari E, Wang H. Therapeutic Role of a Cysteine Precursor, OTC, in Ischemic Stroke Is Mediated by Improved Proteostasis in Mice. *Transl Stroke Res*. 2020;11:147-160. doi: 10.1007/s12975-019-00707-w
17. Liu Y, Min J-W, Feng S, Subedi K, Qiao F, Mammenga E, Callegari E, Wang H. Therapeutic role of a cysteine precursor, OTC, in ischemic stroke is mediated by improved proteostasis in mice. *Translational stroke research*. 2020;11:147-160.

18. Liu Y, Lu L, Hettinger CL, Dong G, Zhang D, Rezvani K, Wang X, Wang H. Ubiquilin-1 protects cells from oxidative stress and ischemic stroke caused tissue injury in mice. *J Neurosci*. 2014;34:2813-2821. doi: 10.1523/JNEUROSCI.3541-13.2014
19. Liu Y, Subedi K, Baride A, Romanova S, Callegari E, Huber CC, Wang X, Wang H. Peripherally misfolded proteins exacerbate ischemic stroke-induced neuroinflammation and brain injury. *J Neuroinflammation*. 2021;18:29. doi: 10.1186/s12974-021-02081-7
20. Min JW, Lü L, Freeling JL, Martin DS, Wang H. USP 14 inhibitor attenuates cerebral ischemia/reperfusion-induced neuronal injury in mice. *Journal of neurochemistry*. 2017;140:826-833.
21. Chen J, Sanberg PR, Li Y, Wang L, Lu M, Willing AE, Sanchez-Ramos J, Chopp M. Intravenous administration of human umbilical cord blood reduces behavioral deficits after stroke in rats. *Stroke*. 2001;32:2682-2688.
22. Asadi Y, Gorjipour F, Behrouzifar S, Vakili A. Irisin peptide protects brain against ischemic injury through reducing apoptosis and enhancing BDNF in a rodent model of stroke. *Neurochemical Research*. 2018;43:1549-1560.
23. Liu Y, Feng S, Subedi K, Wang H. Attenuation of ischemic stroke-caused brain injury by a monoamine oxidase inhibitor involves improved proteostasis and reduced neuroinflammation. *Molecular neurobiology*. 2020;57:937-948.
24. McMillin M, Frampton G, Grant S, Khan S, Diocares J, Petrescu A, Wyatt A, Kain J, Jefferson B, DeMorrow S. Bile acid-mediated sphingosine-1-phosphate receptor 2 signaling promotes neuroinflammation during hepatic encephalopathy in mice. *Frontiers in Cellular Neuroscience*. 2017;11:191.
25. Xu N, Tang X-H, Pan W, Xie Z-M, Zhang G-F, Ji M-H, Yang J-J, Zhou M-T, Zhou Z-Q. Spared nerve injury increases the expression of microglia M1 markers in the prefrontal cortex of rats and provokes depression-like behaviors. *Frontiers in neuroscience*. 2017;11:209.
26. Norwood J, Franklin JM, Sharma D, D'Mello SR. Histone deacetylase 3 is necessary for proper brain development. *Journal of Biological Chemistry*. 2014;289:34569-34582.
27. Liu Y, Qiao F, Leiferman PC, Ross A, Schlenker EH, Wang H. FOXOs modulate proteasome activity in human-induced pluripotent stem cells of Huntington's disease and their derived neural cells. *Hum Mol Genet*. 2017;26:4416-4428. doi: 10.1093/hmg/ddx327
28. Pauleau AL, Rutschman R, Lang R, Pernis A, Watowich SS, Murray PJ. Enhancer-mediated control of macrophage-specific arginase I expression. *J Immunol*. 2004;172:7565-7573. doi: 10.4049/jimmunol.172.12.7565
29. Tang ED, Nunez G, Barr FG, Guan KL. Negative regulation of the forkhead transcription factor FKHR by Akt. *J Biol Chem*. 1999;274:16741-16746. doi: 10.1074/jbc.274.24.16741
30. Brunet A, Bonni A, Zigmond MJ, Lin MZ, Juo P, Hu LS, Anderson MJ, Arden KC, Blenis J, Greenberg ME. Akt promotes cell survival by phosphorylating and inhibiting a Forkhead transcription factor. *Cell*. 1999;96:857-868.
31. Quiros M, Grazulis S, Girdzijauskaite S, Merkys A, Vaitkus A. Using SMILES strings for the description of chemical connectivity in the Crystallography Open Database. *J Cheminform*. 2018;10:23. doi: 10.1186/s13321-018-0279-6
32. Bugnon M, Rohrig UF, Goullieux M, Perez MAS, Daina A, Michielin O, Zoete V. SwissDock 2024: major enhancements for small-molecule docking with Attracting Cavities and AutoDock Vina. *Nucleic Acids Res*. 2024;52:W324-W332. doi: 10.1093/nar/gkae300
33. Meng EC, Goddard TD, Pettersen EF, Couch GS, Pearson ZJ, Morris JH, Ferrin TE. UCSF ChimeraX: Tools for structure building and analysis. *Protein Sci*. 2023;32:e4792. doi: 10.1002/pro.4792

34. Boura E, Rezabkova L, Brynda J, Obsilova V, Obsil T. Structure of the human FOXO4-DBD-DNA complex at 1.9 A resolution reveals new details of FOXO binding to the DNA. *Acta Crystallogr D Biol Crystallogr*. 2010;66:1351-1357. doi: 10.1107/S0907444910042228
35. Liu M, Jia Y, Xie Y, Zhang C, Ma J, Sun C, Ju J. Identification of the Actinomycin D Biosynthetic Pathway from Marine-Derived Streptomyces costaricanus SCSIO ZS0073. *Mar Drugs*. 2019;17. doi: 10.3390/md17040240
36. Hollstein U, Breitmaier E, Jung G. 13-C nuclear jagnetic resonance study of actinomycin D. *J Am Chem Soc*. 1974;96:8036-8040. doi: 10.1021/ja00833a033
37. Santos BF, Grenho I, Martel PJ, Ferreira BI, Link W. FOXO family isoforms. *Cell Death Dis*. 2023;14:702. doi: 10.1038/s41419-023-06177-1
38. Abramson J, Adler J, Dunger J, Evans R, Green T, Pritzel A, Ronneberger O, Willmore L, Ballard AJ, Bambrick J. Accurate structure prediction of biomolecular interactions with AlphaFold 3. *Nature*. 2024;630:493-500.
39. Cui X, Li Z, Yuan Y. Knockdown of FOXO4 protects against OGD/R-induced cerebral microvascular endothelial cell injury and regulates the AMPK/Nrf2/HO-1 pathway through transcriptional activation of CTRP6. *Experimental and Therapeutic Medicine*. 2024;27:1-13.
40. Liu H, Wang L, Weng X, Chen H, Du Y, Diao C, Chen Z, Liu X. Inhibition of Brd4 alleviates renal ischemia/reperfusion injury-induced apoptosis and endoplasmic reticulum stress by blocking FoxO4-mediated oxidative stress. *Redox biology*. 2019;24:101195.
41. Yu L, Zhang W, Huang C, Liang Q, Bao H, Gong Z, Xu M, Wang Z, Wen M, Cheng X. FoxO4 promotes myocardial ischemia-reperfusion injury: the role of oxidative stress-induced apoptosis. *American journal of translational research*. 2018;10:2890.
42. Furuyama T, Kitayama K, Shimoda Y, Ogawa M, Sone K, Yoshida-Araki K, Hisatsune H, Nishikawa S, Nakayama K, Nakayama K, et al. Abnormal angiogenesis in Foxo1 (Fkhr)-deficient mice. *J Biol Chem*. 2004;279:34741-34749. doi: 10.1074/jbc.M314214200
43. Kim JY, Park J, Chang JY, Kim S-H, Lee JE. Inflammation after ischemic stroke: the role of leukocytes and glial cells. *Experimental neurobiology*. 2016;25:241.
44. Qiu Y-m, Zhang C-l, Chen A-q, Wang H-l, Zhou Y-f, Li Y-n, Hu B. Immune cells in the BBB disruption after acute ischemic stroke: targets for immune therapy? *Frontiers in immunology*. 2021;12:678744.
45. Zhu M, Goetsch SC, Wang Z, Luo R, Hill JA, Schneider J, Morris Jr SM, Liu Z-P. FoxO4 promotes early inflammatory response upon myocardial infarction via endothelial Arg1. *Circulation research*. 2015;117:967-977.
46. Caboni L, Lloyd DG. Beyond the ligand-binding pocket: targeting alternate sites in nuclear receptors. *Med Res Rev*. 2013;33:1081-1118. doi: 10.1002/med.21275
47. Zhang JT, Liu JY. Drugging the "undruggable" DNA-binding domain of STAT3. *Oncotarget*. 2016;7:66324-66325. doi: 10.18632/oncotarget.12181
48. Huang W, Dong Z, Chen Y, Wang F, Wang CJ, Peng H, He Y, Hangoc G, Pollok K, Sandusky G, et al. Small-molecule inhibitors targeting the DNA-binding domain of STAT3 suppress tumor growth, metastasis and STAT3 target gene expression in vivo. *Oncogene*. 2016;35:783-792. doi: 10.1038/onc.2015.215
49. Huang W, Dong Z, Wang F, Peng H, Liu JY, Zhang JT. A small molecule compound targeting STAT3 DNA-binding domain inhibits cancer cell proliferation, migration, and invasion. *ACS Chem Biol*. 2014;9:1188-1196. doi: 10.1021/cb500071v

Figure Legend

Fig. 1. Effect of KO of FOXO4 on oxidative stress- and OGD-induced neuronal death in primary neuronal cultures. **a.** Western blot analysis of FOXO4 protein levels in primary neuronal cultures to validate FOXO4 KO. **b.** ATP assay results of KO and WT neurons following MD treatment. **c.** MTT assay results of KO and WT neurons following MD treatment. **d.** ATP assay results of KO and WT neurons following OGD treatment. **e.** MTT assay results of KO and WT neurons following OGD treatment. Data are shown as mean ± SD. N = 10-14, ***p < 0.001. ns, no significant difference.

Fig. 2. KO of FOXO4 reduces brain infarct volume, improves animal survival, and enhances functional recovery following I/R. a. Western blot analysis of FOXO4 protein levels in mouse brain to validate FOXO4 KO. **b.** A schematic of experimental design. **c.** Representative TTC staining of mouse brains from the sham surgery, WT, and KO animal groups after MCAO. **d.** Quantitation of TTC staining results. **e.** KO mice increased the animal survival rate compared to WT mice after tMCAO. **f.** KO mice improved mNSSs compared to WT mice after tMCAO. **g.** KO mice showed better memory compared to WT mice in the NOR test after tMCAO. Data are shown as mean ± SD. N = 10-14 for **(d)**, ****p < 0.0001. N = 14– 15 for (**e**)-(**g**), * p < 0.05, **p < 0.01, ***p < 0.001.

Fig. 3. KO of FOXO4 attenuates neuroinflammation following I/R. **a.** Representative western blot results of the indicated proteins. **b-d.** Quantified results of the indicated proteins. Data are shown as mean ± SEM, * p < 0.05, **p < 0.01.

Fig. 4. FOXO4 KO mouse brains showed reduced astrocytes and microglia two days after I/R compared to WT mouse brains. a. Representative images showing GFAP staining in the WT and FOXO4 KO brains. Scale bar, 50 µm. **b.** Representative images showing Iba1 staining in the WT and FOXO4 KO brain sections following I/R. Scale bar, 50 µm. **c.** Quantitation of GFAP positively stained cells (green). **d.** Quantitation of Iba1 positively stained cells (red). All numeric data are shown as mean ± SD; n = 7 for each group. *p < 0.05, **p < 0.01.

Fig. 5. FOXO4 KO brain shows reduced leukocyte infiltration following I/R. a. Representative image showing CD45 staining. **b.** Quantitation of CD45-positively stained cells in the brain. **c.** Representative image showing CD11b staining. **d.** Quantitation of CD11b-positively stained cells. **e.** Representative image showing Ly6G staining. **f.** Quantitation of Ly6G-positively stained cells. Scale bar, 50 µm. Data are shown as mean ± SD; n = 5-7 for each group. ns, no significant difference; *p < 0.05, ***p < 0.001.

Fig. 6. Identification of ActD as a FOXO4 inhibitor. a. Structure of the FOXO4 DBD–DNA complex. The FOXO-DBD is shown in blue ribbon (upper) and the DNA double helix is shown as orange and green (*lower*) (https://www.rcsb.org/structure/3L2C). **b.** Structure of ActD. **c.** The result of a luciferase reporter assay shows that ActD inhibited FOXO4 activity. **d.** The result of a luciferase reporter assay shows that ActD did not inhibit FOXO3 activity. **e & f.** The results of computational protein-ligand docking advocated helix H3 as the major site of inhibition. **g.** SwissDock-based AutoDock Vina execution exhibited active residues Arg78, His79 and Ser82 interacting with ActD. **h.** AlphaFold3-based Protenix predicted similar heavy atom contacts with ligand to H2 (Leu47), H3 (Asn75, Arg78, His79, Ser82 and Leu83) and S3 (Lys89) domains of FOXO4. All numerical data are shown as mean ± SD. N = 3, *p <0.05, ns, no significant difference.

Fig. 7. Effect of ActD on oxidative stress- and OGD-induced neuronal death in the WT primary neuronal cultures. **a.** ATP assay results of WT neurons treated with 20 µM of MD in the presence of 0.1 µM of ActD. **b.** MTT assay results of WT neurons treated with 20 µM of MD in the presence of 0.1 µM of ActD. **d.** ATP assay results of WT neurons treated with OGD in the presence of 0.1 µM of ActD. **e.** MTT assay results of WT neurons treated with OGD in the presence of 0.1 µM of ActD. Data are shown as mean ± SD. N = 10-14, *p <0.05, **p < 0.01, ***p < 0.001, ****p < 0.0001.

Fig 8. Effect of ActD on I/R-indued brain injury in the WT following tMCAO. a. A **b.** A schematic of experimental design. **b.** Representative TTC staining of mouse brains from the sham surgery, vehicle-treated, and ActD (0.25 or 0.5 mg/kg)-treated mouse brains after MCAO. **c.** Quantitation of TTC staining results. **d.** ActD improved mNSSs compared to vehicle-treated mice after tMCAO. **e.** ActD-treated mice showed better memory compared to vehicle-treated mice in the Y-maze test after tMCAO. Data are shown as mean ± SD. N = 12 for (**c**); n = 14-15 for (**d & e**); *p < 0.05, **p < 0.01, ****p < 0.0001.

Fig. 1

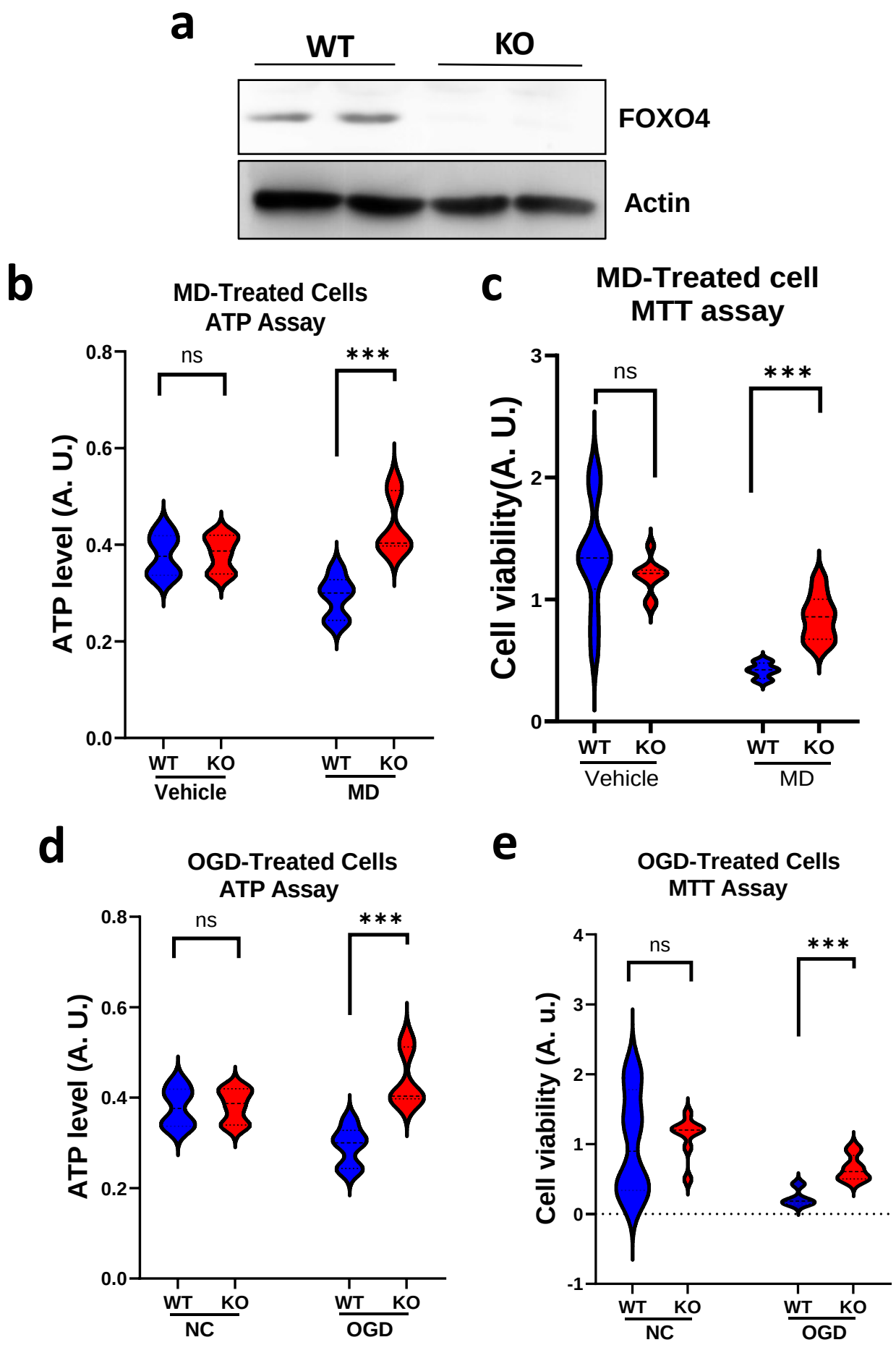
a
WT
KO
FOXO4
Actin
b
MD-Treated Cells
ATP Assay
ATP level (A. U.)
0.8
0.6
0.4
0.2
0.0
ns
***
WT
KO
WT
KO
Vehicle
MD
c
MD-Treated cell
MTT assay
Cell viability(A. U.)
3
2
1
0
ns
***
WT
KO
WT
KO
Vehicle
MD
d
OGD-Treated Cells
ATP Assay
ATP level (A. U.)
0.8
0.6
0.4
0.2
0.0
ns
***
WT
KO
WT
KO
NC
OGD
e
OGD-Treated Cells
MTT Assay
Cell viability (A. u.)
4
3
2
1
0
-1
ns
***
WT
KO
WT
KO
NC
OGD

Fig. 2

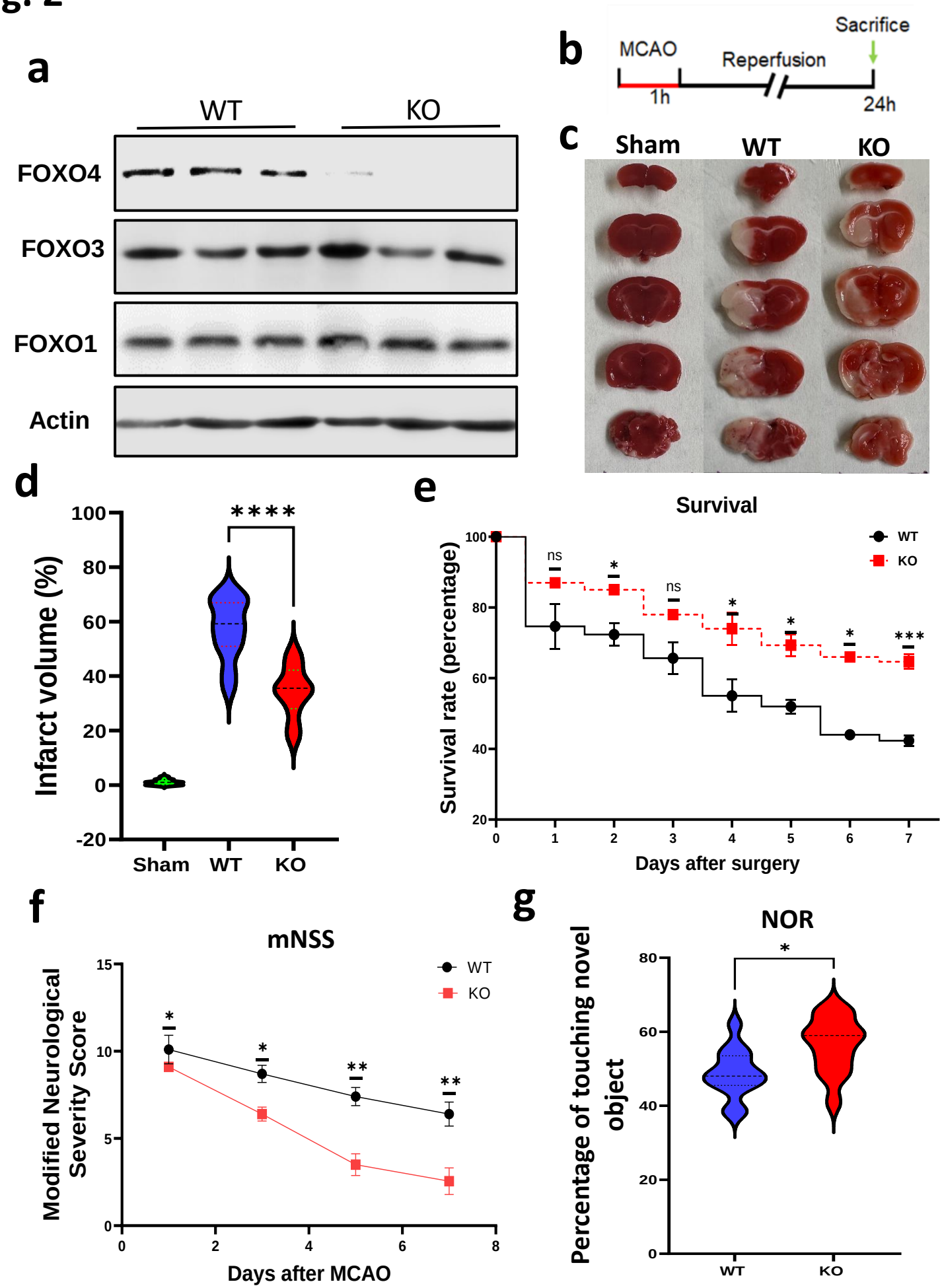
a
WT
KO
FOXO4
FOXO3
FOXO1
Actin
b
MCAO
Reperfusion
Sacrifice
1h
24h
c
Sham
WT
KO
d
Infarct volume (%)
****
Sham
WT
KO
e
Survival
Survival rate (percentage)
Days after surgery
WT
KO
ns
*
ns
*
*
*
***
f
mNSS
Modified Neurological Severity Score
Days after MCAO
WT
KO
*
*
**
**
g
NOR
Percentage of touching novel object
*
WT
KO

Fig. 3

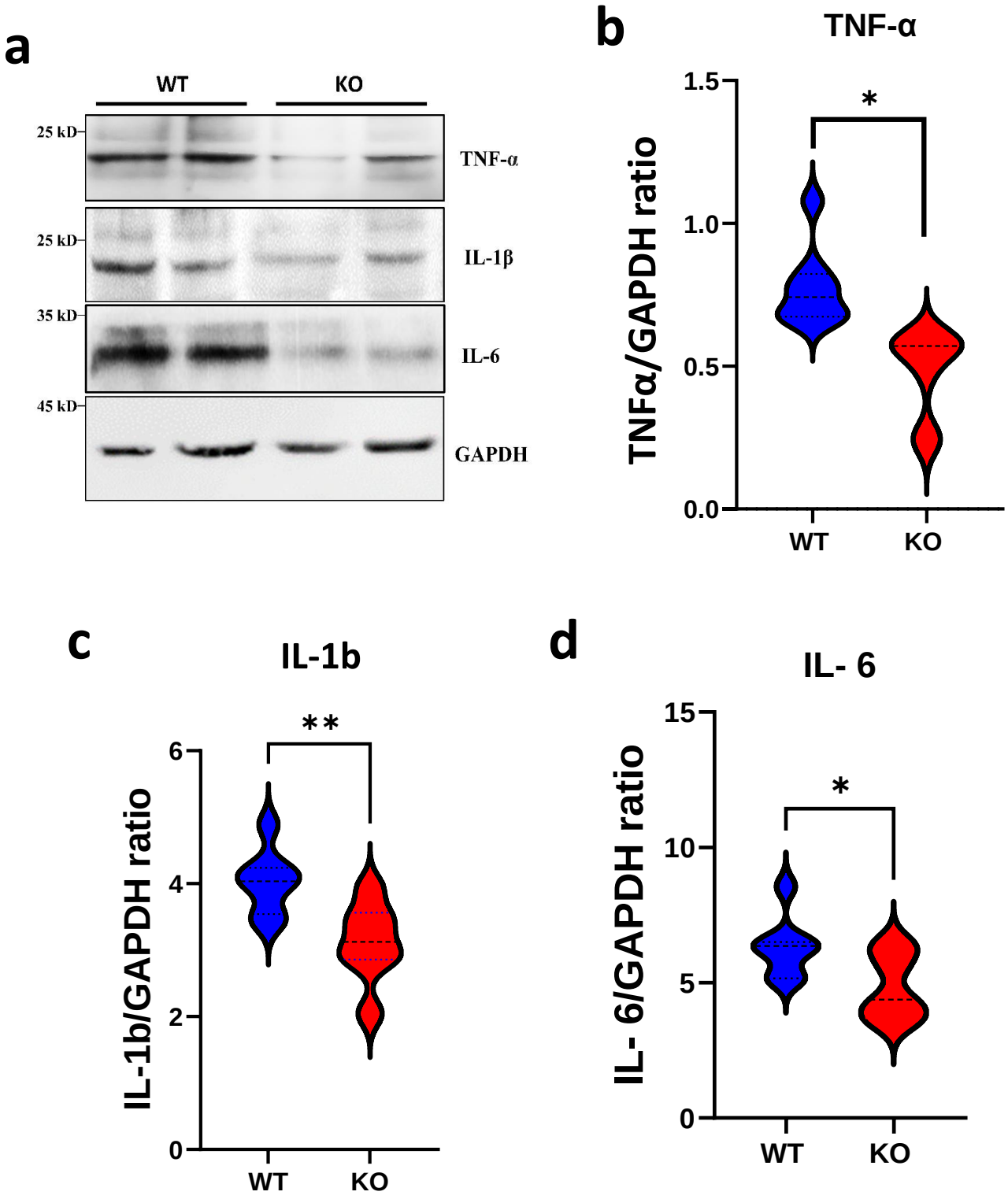
a
WT
KO
25 kD
TNF-α
25 kD
IL-1β
35 kD
IL-6
45 kD
GAPDH
b
TNF-α
TNFα/GAPDH ratio
1.5
1.0
0.5
0.0
*
WT
KO
c
IL-1b
IL-1b/GAPDH ratio
6
4
2
0
**
WT
KO
d
IL- 6
IL- 6/GAPDH ratio
15
10
5
0
*
WT
KO

Fig. 4

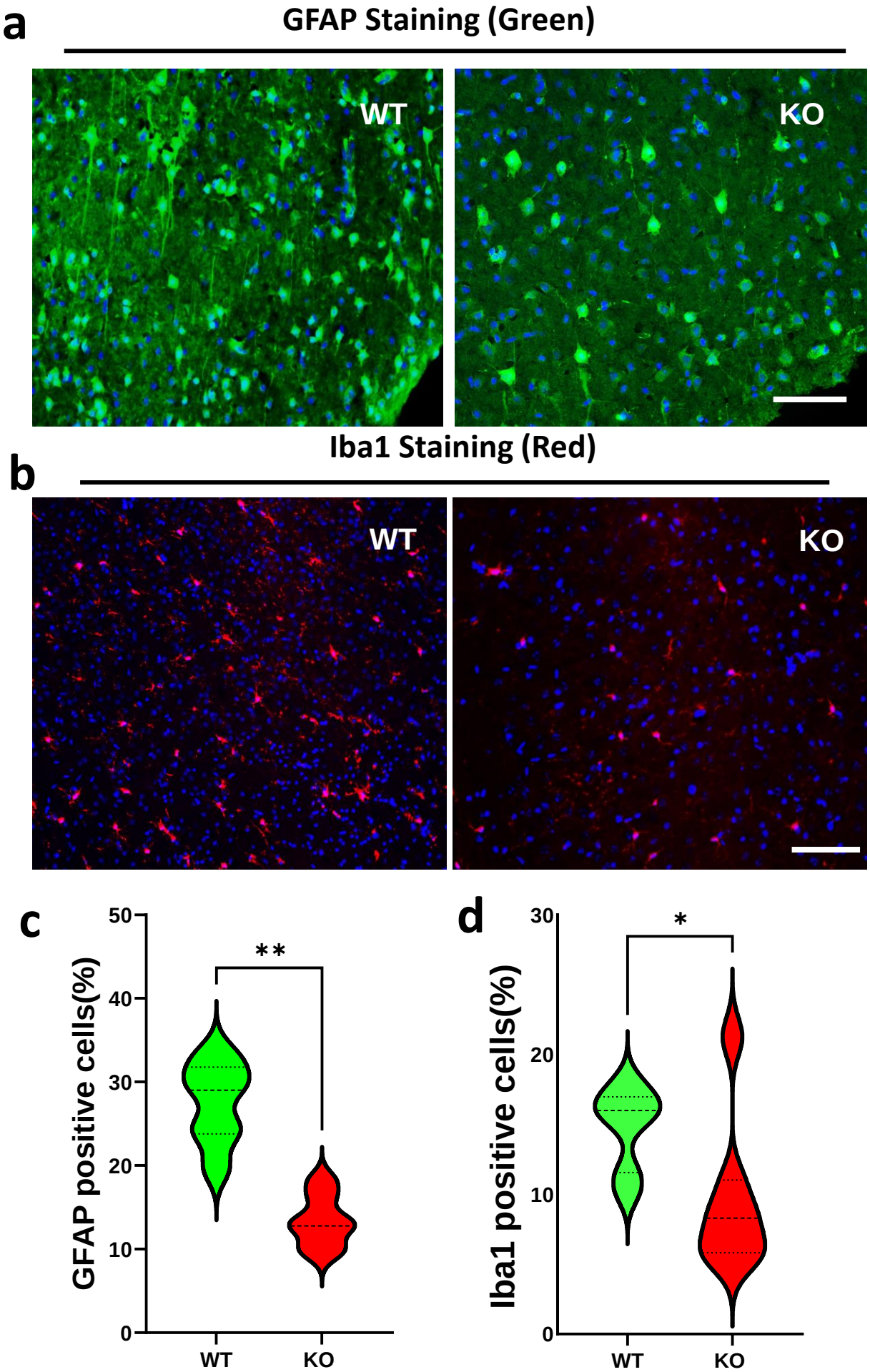
a
GFAP Staining (Green)
WT
KO
b
Iba1 Staining (Red)
WT
KO
c
GFAP positive cells(%)
50
40
30
20
10
0
**
WT
KO
d
Iba1 positive cells(%)
30
20
10
0
*
WT
KO

Fig. 5

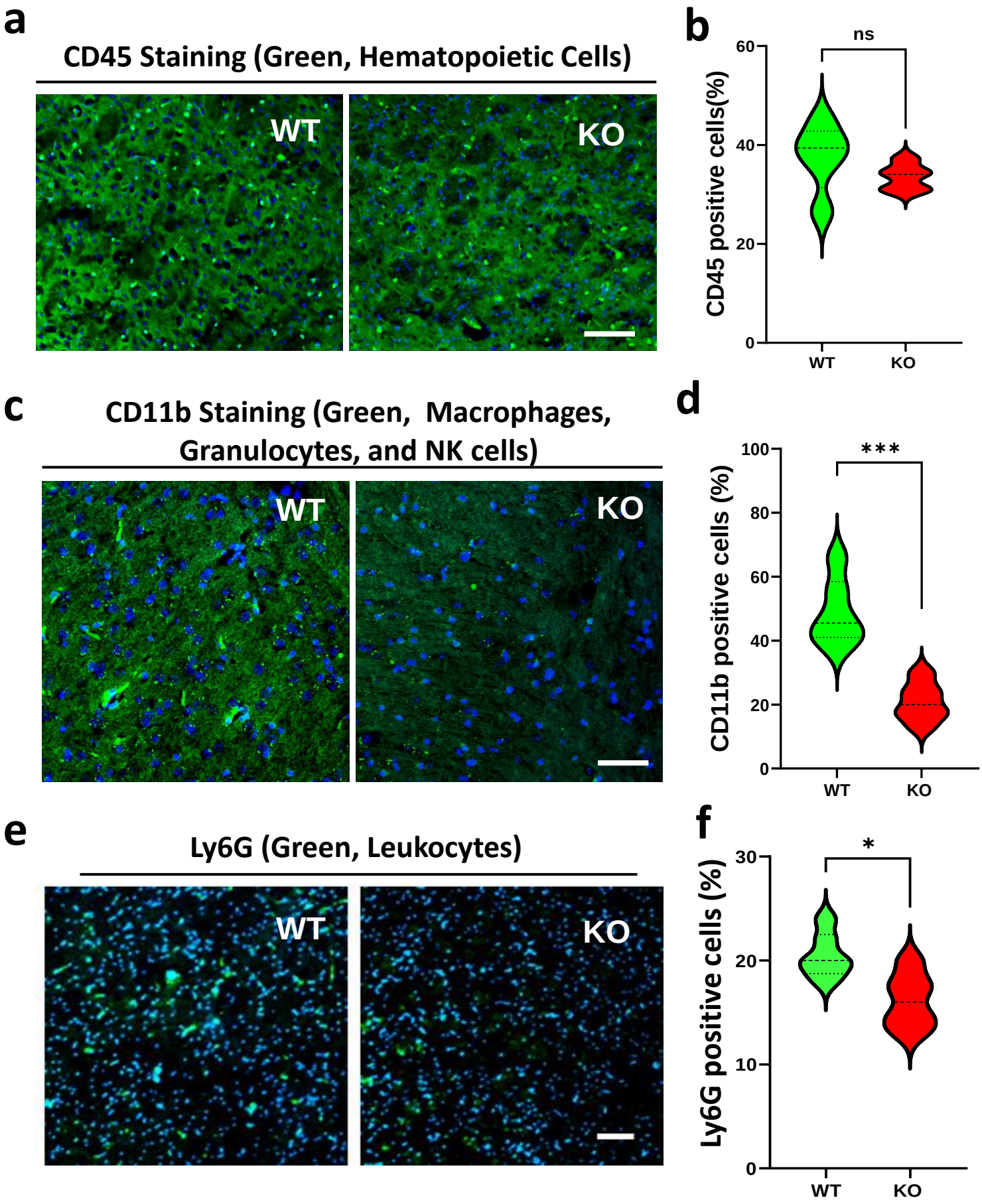
a
CD45 Staining (Green, Hematopoietic Cells)
WT
KO
b
ns
CD45 positive cells(%)
60
40
20
0
WT
KO
c
CD11b Staining (Green, Macrophages, Granulocytes, and NK cells)
WT
KO
d
***
CD11b positive cells (%)
100
80
60
40
20
0
WT
KO
e
Ly6G (Green, Leukocytes)
WT
KO
f
*
Ly6G positive cells (%)
30
20
10
0
WT
KO

Fig. 6

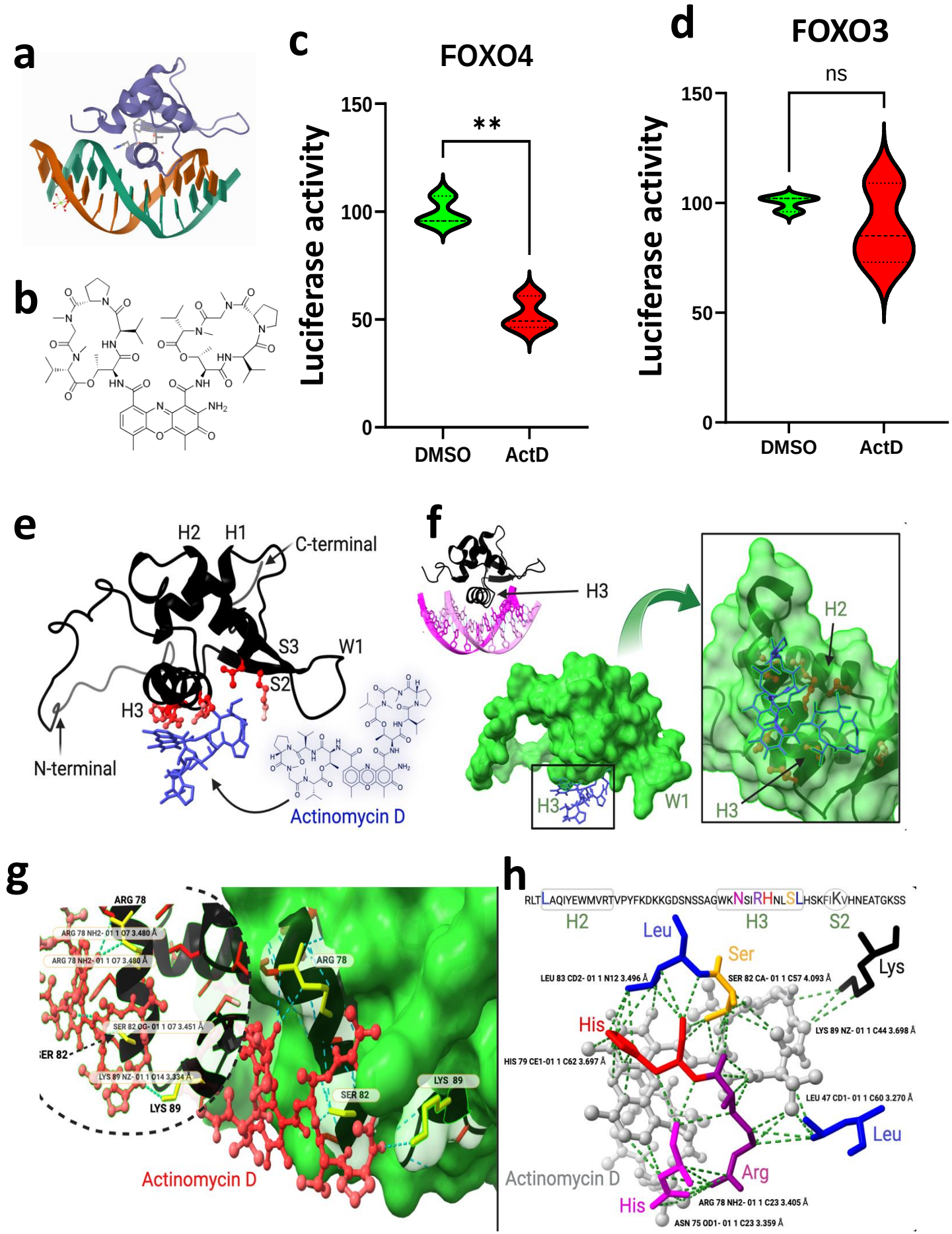
a
b
c
FOXO4
Luciferase activity
150
100
50
0
**
DMSO
ActD
d
FOXO3
ns
Luciferase activity
150
100
50
0
DMSO
ActD
e
H2
H1
C-terminal
S3
W1
S2
H3
N-terminal
Actinomycin D
f
H3
H2
H3
W1
H3
g
ARG 78
ARG 78 NH2- 01 1 O7 3.480 Å
ARG 78 NH2- 01 1 O7 3.480 Å
SER 82 OG- 01 1 O7 3.451 Å
SER 82
LYS 89 NZ- 01 1 O14 3.334 Å
LYS 89
ARG 78
SER 82
LYS 89
Actinomycin D
h
RLTLAQIYEWMVRTVPYFKDKKGDSNSSAGWKNSIRHNLSLHSKFIKVHNEATGKSS
H2
H3
S2
Leu
Ser
Lys
LEU 83 CD2- 01 1 N12 3.496 Å
SER 82 CA- 01 1 C57 4.093 Å
His
LYS 89 NZ- 01 1 C44 3.698 Å
HIS 79 CE1-01 1 C62 3.697 Å
LEU 47 CD1- 01 1 C60 3.270 Å
Leu
Actinomycin D
Arg
His
ARG 78 NH2- 01 1 C23 3.405 Å
ASN 75 OD1- 01 1 C23 3.359 Å

Fig. 7

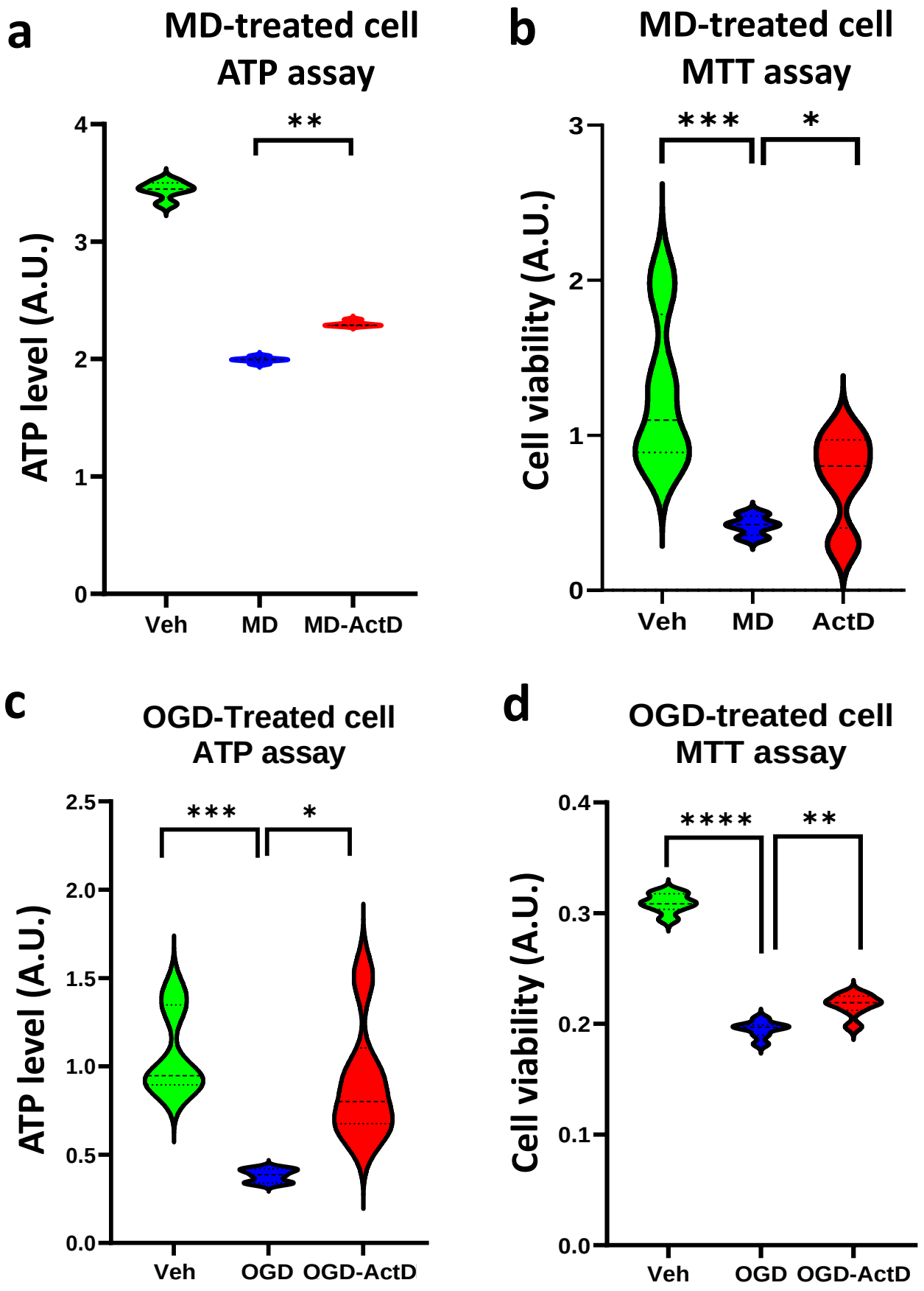
a
MD-treated cell
ATP assay
ATP level (A.U.)
4
3
2
1
0
**
Veh
MD
MD-ActD
b
MD-treated cell
MTT assay
Cell viability (A.U.)
3
2
1
0
***
*
Veh
MD
ActD
c
OGD-Treated cell
ATP assay
ATP level (A.U.)
2.5
2.0
1.5
1.0
0.5
0.0
***
*
Veh
OGD
OGD-ActD
d
OGD-treated cell
MTT assay
Cell viability (A.U.)
0.4
0.3
0.2
0.1
0.0
****
**
Veh
OGD
OGD-ActD

Fig. 8

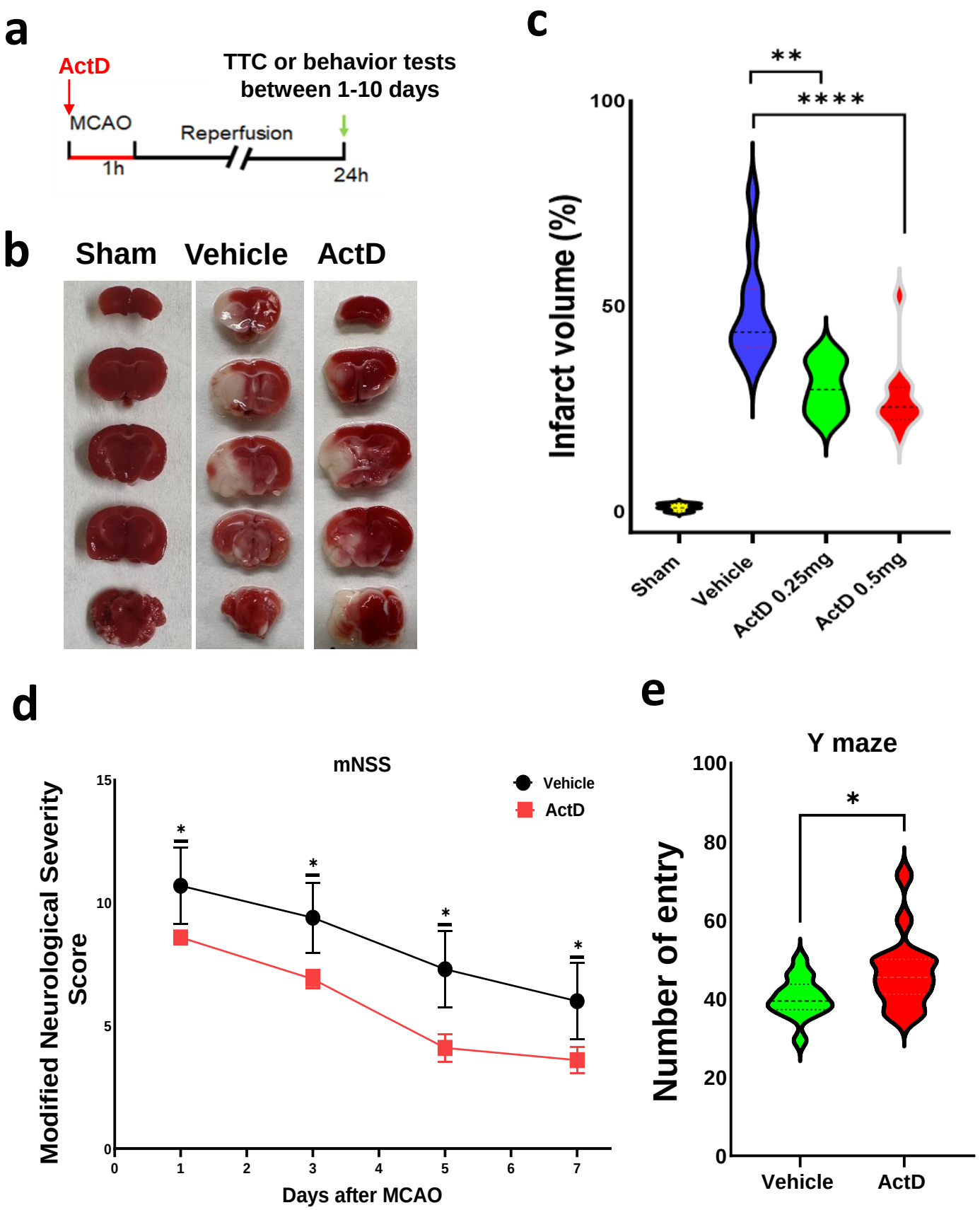
a
ActD
TTC or behavior tests
between 1-10 days
MCAO
Reperfusion
1h
24h
b
Sham
Vehicle
ActD
c
Infarct volume (%)
100
50
0
**
****
Sham
Vehicle
ActD 0.25mg
ActD 0.5mg
d
mNSS
Vehicle
ActD
Modified Neurological Severity Score
15
10
5
0
*
0
1
2
3
4
5
6
7
Days after MCAO
e
Y maze
Number of entry
100
80
60
40
20
0
*
Vehicle
ActD